Redox Biology 84 (2025) 103670

Contents lists available at ScienceDirect

Redox Biology

journal homepage: www.elsevier.com/locate/redox

Development of SOCS1 mimetics as novel approach to harmonize inflammation, oxidative stress, and fibrogenesis in metabolic dysfunction-associated steatotic liver disease

Susana Bernal [a,b,1], Ignacio Prieto [a,b,1], María Kavanagh [a,b,1], Isabel Herrero del Real [a], Sara La Manna [c], Iolanda Lázaro [d,e], Hernán Quiceno [f], Laura López-Sanz [a,b], Belén Picatoste [a,g], M. Pilar Valdecantos [h,b], Sebastián Mas-Fontao [a,b], Aleix Sala-Vila [d,e], Ángela M. Valverde [h,b], Daniela Marasco [c], Jesús Egido [a,b], Carmen Gómez-Guerrero [a,b,*]

[a] Renal, Vascular and Diabetes Research Lab, IIS-Fundación Jiménez Díaz, Autonomous University of Madrid (IIS-FJD/UAM), Madrid, 28040, Spain
[b] Diabetes and Associated Metabolic Diseases Networking Biomedical Research Centre (CIBERDEM), Madrid, 28029, Spain
[c] Department of Pharmacy, University of Naples Federico II, Naples, 80131, Italy
[d] Hospital del Mar Medical Research Institute, Barcelona, 08003, Spain
[e] Physiopathology of Obesity and Nutrition Networking Biomedical Research Centre (CIBEROBN), Madrid, 28029, Spain
[f] Department of Pathology, IIS-Fundación Jiménez Díaz, Madrid, 28040, Spain
[g] Hepatic and Vascular Diseases Lab. Biochemistry and Molecular Biology Department. School of Pharmacy, Complutense University of Madrid, Madrid, 28040, Spain
[h] Institute for Biomedical Research Sols-Morreale (IIBM), Spanish National Research Council- Autonomous University of Madrid (CSIC-UAM), Madrid, 28029, Spain

ARTICLE INFO

Keywords:
MASLD
Steatosis
Oxidative stress
Inflammation
Fibrosis
JAK/STAT

ABSTRACT

Background: Metabolic dysfunction-associated steatotic liver disease (MASLD) is a prevalent chronic liver disease, encompassing a spectrum from simple steatosis to steatohepatitis (MASH), cirrhosis, and hepatocellular carcinoma. As part of metabolic syndrome, MASLD/MASH is characterized by inflammation, oxidative stress, and fibrosis, highlighting the need for targeted therapies. The dysregulation of Janus kinase/signal transducers and activators of transcription (JAK/STAT) pathway and its negative regulators the suppressors of cytokine signaling (SOCS), plays a critical role in liver function and contributes to MASLD progression.

Aim: Based on a SOCS1 functional domain, we developed mimetic peptides (linear and cyclic) targeting JAK activity and assessed their hepatoprotective potential in experimental MASLD/MASH.

Results: In dietary mouse models of MASLD/MASH, the administration of peptides ameliorated liver damage at both early and advanced stages, as evidenced by significant decreases in serum transaminases and hepatic content of lipids, inflammatory cells, and collagen. Treatment attenuated hepatic STAT1/3 activation and downregulated genes involved in inflammation, fibrosis, and lipid metabolism. Livers from treated mice exhibited lower levels of oxidative damage markers, reduced expression of NADPH oxidase 1 (NOX1), and upregulation of the antioxidant genes catalase and superoxide dismutase. In vitro, the peptides were safe for

Abbreviations: ABCA/G, ATP-binding cassette subfamily A/G; ACTA2, α-smooth muscle actin; ALT/AST, alanine/aspartate aminotransferase; APOE, Apolipoprotein E; ARG, Arginase; CAT, catalase; BSA, Bovine serum albumin; CCL/CXCL, CC/CXC Motif Chemokine Ligand; CHOP, DNA-damage inducible transcript-3; COL1A, Collagen type Iα1; CPT1a, Carnitine palmitoyltransferase-1α; ECM, Extracellular matrix; ER, Endoplasmic reticulum; FA, Fatty acid; FABP1, Fatty acid-binding protein-1; FASN, Fatty acid synthase; FBS, Fetal bovine serum; HFD, High-fat diet; 4HNE, 4-hydroxynonenal; HSC, Hepatic stellate cells; IL, Interleukin; JAK/STAT, Janus kinase/signal transducers and activators of transcription; KIR, Kinase inhibitory region; NAFLD, non-alcoholic fatty liver disease; MASLD/MASH, Metabolic dysfunction-associated steatotic liver disease/steatohepatitis; MCD, Methionine-choline-deficient; MMP, Matrix metallopeptidase; MTT, 3-(4,5-dimethylthiazol-2-yl)-2,5-diphenyltetrazolium bromide tetrazolium; NOS2, Nitric oxide synthase-2; NOX, NADPH oxidase; 8OHdG, 8-hydroxy-2′-deoxyguanosine; ORO, Oil-Red-O; PPARGC1α, Peroxisome proliferator-activated receptor gamma coactivator 1α; ROS, Reactive oxygen species; SOCS, Suppressors of cytokine signalling; SOD, Superoxide dismutase; SREBF1, Sterol regulatory element-binding transcription factor-1; TG, Triglycerides; TGFβ, Transforming growth factor-β1; TIMP1, Tissue inhibitor of metalloproteinase-1; TNFα, Tumor necrosis factor-α.

* Corresponding author. Renal, Vascular and Diabetes Research Lab. IIS-Fundación Jiménez Díaz, Autonomous University of Madrid (IIS-FJD/UAM). Avda Reyes Catolicos 2. Madrid, 28040, Spain.
E-mail addresses: c.gomez@uam.es, cgomez@fjd.es (C. Gómez-Guerrero).
[1] These authors contribute equally.

https://doi.org/10.1016/j.redox.2025.103670
Received 24 January 2025; Received in revised form 28 April 2025; Accepted 10 May 2025
Available online 11 May 2025

hepatocytes at different doses and effectively counteracted palmitate-induced cytotoxicity, superoxide anion production, and cytokine and NOX1 expression, while increasing anti-inflammatory and antioxidant genes.
Conclusions: SOCS1 mimetic peptides exhibit hepatoprotective effects in experimental MASLD/MASH by modulating lipotoxicity, inflammation, redox balance and fibrogenesis. This proof-of-concept supports their potential as candidates for preclinical MASLD therapy development.

1. Introduction

Metabolic dysfunction-associated steatotic liver disease (MASLD), formerly named non-alcoholic fatty liver disease (NAFLD), is a common chronic liver condition affecting 32 % of adults worldwide, frequently associated with obesity, type 2 diabetes and dyslipidemia [1]. MASLD ranges from simple steatosis to metabolic dysfunction-associated steatohepatitis (MASH), a progressive subtype associated with higher morbidity, mortality and cardiovascular risk [2], characterized by lipid accumulation, hepatocyte injury, inflammation, and fibrosis that can progress to cirrhosis, liver failure, and hepatocellular carcinoma [3].

MASLD progression involves a cascade of "multiple hits" derived from gut, adipose tissue, and liver [4], including lipid and glucose metabolism alterations and insulin resistance, leading to the release of inflammatory mediators and reactive oxygen species (ROS), mitochondrial dysfunction, and endoplasmic reticulum (ER) stress. These harmful factors trigger several signaling pathways that ultimately perpetuate inflammation and promote hepatocyte death, hepatic stellate cells (HSC) activation, and extracellular matrix (ECM) deposition, all hallmarks of MASH [3,5].

No specific medical therapies exist for MASLD, except for the recent approval of resmetirom for non-cirrhotic MASH [6]. Lifestyle modifications remain the primary intervention, with adjunctive treatments like vitamin E or pioglitazone. Ongoing clinical trials are exploring drugs targeting metabolism, such as fatty acid (FA) synthesis inhibitors, incretin-based therapies, and peroxisome proliferator-activated receptor agonists. Investigational drugs targeting inflammation and fibrosis are in development stages [7,8]. Understanding the mechanisms driving MASLD and MASH is crucial for developing effective therapies and improving patient outcomes.

The Janus kinase/signal transducer and activator of transcription (JAK/STAT) transduces signals from metabolically relevant molecules like hormones, lipids, and cytokines. Its overactivation is linked to insulin resistance, lipid dysfunction, immune responses, and tumor development [9]. In MASLD/MASH, JAK/STAT regulates macrophage functions, hepatocyte survival and regeneration, and HSC activation via cytokine and fibrogenic molecule expression [10,11]. Negative feedback regulation of JAK/STAT is achieved by the suppressors of cytokine signaling (SOCS). SOCS1, the main family member, inactivates JAK through competitive inhibition via its kinase inhibitory region (KIR), counteracting STAT1/STAT3-driven transcription, and regulating inflammation and oxidative stress [12]. Functional SOCS1 polymorphisms associate with obesity and MASLD [13]. SOCS1 inhibition in animal models worsens hepatic damage [14–16] and tumor development [17], highlighting its protective role in the liver.

We previously tested SOCS1 peptidomimetics for therapeutic use. Lead compound S1, mimicking the SOCS1 KIR domain, showed protective effects in experimental atherothrombosis and nephropathy [18–21]. New mimetics (liPS, IC, and ICNal) demonstrated improved affinity, stability, and anti-inflammatory properties in vitro [22–24]. In the present work we investigate, for the first time, the ability of this family of SOCS1 mimetics to suppress hepatic JAK/STAT activation in vitro and in vivo, and to alleviate MASLD/MASH progression in two dietary mouse models.

2. Material and methods

2.1. Peptide synthesis

Lead compound S1, derived from SOCS1 KIR region (53–68), and new mimetics comprising a linear sequence with acetaminomethylcysteine substitution (liPS) and two cyclopeptides with a side-chain lactam bridge and additional 3-(1-naphthyl)-alanine substitution (IC and ICNal) were synthesized (ProteoGenix, Schiltigheim, France; KareBay Biochem, Monmouth Junction, NJ, USA) and structural characterized as previously reported [18,23,24]. Chemical structures and lipophilicity profiles of peptides are shown in Supplementary Figs. S1 and S2, respectively. S1 was conjugated to palmitoyl-lysine for cell-permeability and initially dissolved in 3 % DMSO. LiPS, IC and ICNal were conjugated to the 48–60 fragment of the HIV-1 transactivator of transcription and dissolved in saline.

2.2. Experimental mouse models

Animal procedures conformed to ARRIVE Guidelines and Directive 2010/63/EU of the European Parliament and were approved by the Institutional Animal Care and Use Committee of IIS-Fundación Jiménez Díaz and Comunidad de Madrid (PROEX 217/19 and 128.4/23). Male C57BL/6J mice (Charles River Laboratories, France) and apolipoprotein E-deficient (*ApoE*$^{-/-}$) mice (Jackson Laboratory, Bar Harbor, ME, USA) were maintained in ventilated cages (2–4 mice per cage) with controlled temperature (20–22 °C), a 12-h light/dark cycle, and free access to food and water.

In the first experiment, 20-week-old C57BL/6J mice (n = 32) were fed a methionine-choline-deficient (MCD) diet (TD.90262; Envigo, Indianapolis, IN, USA) for 3 weeks and were randomized to receive S1 or liPS at two different doses (0.6 and 1.2 nmol/g body weight, intraperitoneally, 3 times weekly) or vehicle (<0.5 % DMSO) as a control group. Peptide and vehicle doses were based on our previous experiments that demonstrated no adverse effects on mice [18,20,23]. In the second experiment, C57BL/6J mice (n = 36) on a 3-week MCD diet were randomized into a control untreated group and four treatment groups (S1, liPS, IC or ICNal; 1.2 nmol/g) while continuing MCD diet feeding for another 3 weeks. In the third experiment, 12-week-old *ApoE*$^{-/-}$ mice (n = 48) were placed on a high-fat western diet (HFD; Envigo TD.88137) and untreated or treated with S1, liPS, IC or ICNal (1.2 nmol/g) for 12 weeks. Age-matched mice on a normal chow diet (ND) served as reference groups (n = 7–8).

Animals were monitored weekly for body weight and blood glucose, as well as for clinical signs of toxicity, including abnormal behavior and changes in the appearance of urine, stool, or fur. A glucose tolerance test was performed on 12h-fasted *ApoE*$^{-/-}$ mice (at 11 weeks of HFD) by measuring blood glucose levels from tail vein samples at 0–120 min following an intraperitoneal glucose injection (1 mg/g). At the end of the study, 12h-fasted mice were anesthetized (100 mg/kg ketamine and 15 mg/kg xylazine) and saline-perfused, then blood and liver were collected post-euthanasia.

For single-dose pharmacokinetics, mice (n = 3/group) were injected intraperitoneally with carboxytetramethylrhodamine-labeled peptides, and plasma and urine samples were collected at different times as previously described [19]. Fluorescence intensity was directly measured in 20 μl of sample using a Tecan Infinity M Plex (λemission = 540 nm; λexcitation = 570 nm), and the signal was normalized to initial

fluorescence and body weight. Plasma half-lives were calculated using a one-phase exponential decay model.

2.3. Biochemical and hepatic lipid analysis

Serum alanine aminotransferase (ALT) and aspartate aminotransferase (AST) were measured using a spectrophotometric activity assay (Reflotron, Roche). Serum triglycerides (TG) and total cholesterol were determined by enzymatic colorimetric assays (11528; BioSystems, Barcelona, Spain; STA-384; Cell Biolabs, San Diego, CA, USA). Total hepatic lipids were extracted from homogenized tissue (10–20 mg) by Folch method [25]. Cholesterol and TG concentration were determined by colorimetric assay. Finally, TG and non-esterified FA fractions were isolated from liver homogenates by lipid extraction followed by solid-phase extraction. FA methyl esters of each fraction were obtained by transmethylation and further determined by gas chromatography/electron ionization-mass spectrometry. Concentrations were normalized to liver tissue weight [26].

2.4. Liver histopathology

Formalin-fixed liver samples were paraffin embedded, and 4-μm sections were stained with hematoxylin/eosin. Samples were blindly evaluated for MASLD/NAFLD activity score (encompassing steatosis, lobular inflammation and hepatocyte ballooning) by an experienced liver pathologist, according to mouse criteria [27]. For immunohistochemistry, paraffin sections were incubated with antibodies against macrophages (F4/80; Bio-Rad Cat# MCA497, RRID:AB_2098196), T-cells (CD3; Agilent Cat# A0452, RRID:AB_2335677), 8-hydroxy-2′-deoxyguanosine (8OHdG; Abcam Cat# ab48508, RRID:AB_867461), 4-hydroxynonenal (4HNE; Abcam Cat# ab46545, RRID:AB_722490) and phosphorylated STATs (P-STAT1 (Y701), Thermo Fisher Scientific Cat#44–376, RRID:AB_2533642; P-STAT3 (S727), Cell Signaling Technology Cat# 9134, RRID:AB_331589), followed by respective secondary antibodies conjugated to either horseradish peroxidase or biotin (Jackson Immunoresearch, West Grove, PA, USA) plus avidin-biotin complex (PK-4000; Vector Laboratories, Burlingame, CA, USA), and color development with 3,3′-diaminobenzidine. Liver fibrosis was assessed by Sirius red staining. Oil-Red-O (ORO) staining was performed on frozen 7-μm liver sections. Positive staining in captured images (6–8 fields at 10X magnification; 2 slices/mice) was quantified using Image-Pro Plus software (Media Cybernetics, Bethesda, MD, USA) and expressed as percentage of total area.

2.5. Cell culture and stimulation

Palmitic acid complexed to FA-free bovine serum albumin (BSA) (Sigma-Aldrich, St. Louis, MO, USA) in a 2:1 M ratio, was prepared as described [28]. Immortalized neonatal mouse hepatocytes [29] were cultured in DMEM with 10 % fetal bovine serum (FBS), 2 mM L-glutamine, 100 U/mL penicillin and 100 μg/mL streptomycin (Sigma-Aldrich). Cells were starved overnight in low serum (0.5 % FBS) medium, then treated with different concentrations of mimetic peptides for 90 min before stimulation with 0.4 mM palmitic acid for additional 6–24 h. The palmitic concentration aligns with levels found in MASLD patients [30]. BSA was used as negative control. In some experiments, hepatocyte conditioned medium was collected, centrifuged to remove cell debris, and stored at −20 °C. Mouse macrophage RAW 264.7 cells (ATCC Cat# TIB-71, RRID:CVCL_0493) were plated on 6-well plates (1×10^6 cells/well) in DMEM with 10 % FBS, serum-deprived overnight, and then incubated with hepatocyte conditioned medium for 24 h.

2.6. Cell viability, lipid content and ROS measurement

Hepatocytes on 96-well plates (1×10^4 cells/well) were incubated with palmitic acid with/without peptides. After 24 h, cells were stained with 3-(4,5-dimethylthiazol-2-yl)-2,5-diphenyltetrazolium bromide tetrazolium (MTT; 0.5 mg/mL, Sigma-Aldrich) for 60 min at 37 °C. The resulting formazan crystals were dissolved in DMSO, and absorbance was measured at 570 nm.

For intracellular lipid staining, hepatocytes on 8-well chambers were fixed in 10 % paraformaldehyde, treated with 60 % isopropanol, and incubated with ORO solution for 5 min, then washed and counterstained with hematoxylin.

NADPH oxidase (NOX)-dependent ROS generation was measured by lucigenin chemiluminescence assay [31]. Cell homogenates were mixed with 5 μM lucigenin and 100 μM NADPH (Sigma-Aldrich), then chemiluminescence was recorded in a Berthold luminometer at 10-s intervals for 10 min and normalized to protein content. The NOX inhibitor apocynin (3 mM; Sigma-Aldrich) was used as control.

2.7. Protein analysis

Protein lysates (30–35 μg) from homogenized livers and cells were electrophoresed and immunoblotted for P-STAT1 (Thermo Fisher Scientific Cat# 33–3400, RRID:AB_2533113), STAT1 (Cell Signaling Technology Cat# 9172, RRID:AB_2198300), P-STAT3 (Cell Signaling) and STAT3 (Cell Signaling Technology Cat# 9139, RRID:AB_331757), with β-actin (Sigma-Aldrich Cat# A1978, RRID:AB_476692) and α-tubulin (Sigma-Aldrich Cat# T9026, RRID:AB_477593) as loading controls. STAT1 activation was assessed by modified cellular ELISA using P-STAT1 or total STAT1 antibodies as previously described [32]. Protein concentrations of CC Motif Chemokine Ligand 2 (CCL2) and tumor necrosis factor-α (TNFα) in cell supernatants were measured by ELISA (DY479 and DY410; R&D Systems, MN, USA).

2.8. Quantitative real-time PCR (qPCR) analysis

Total mRNA from livers and cells was extracted using TRI Reagent (Thermo Fisher Scientific). Complementary DNA was synthesized (High-Capacity cDNA Reverse Transcription Kit; 4368813, Applied Biosystems, Foster City, CA, USA) and analyzed by qPCR using Premix Ex Taq (RR390; Takara, Shiga, Japan). TaqMan mouse gene expression assays (Thermo Fisher Scientific) are detailed in Supplementary Table S1. Expression data were normalized to 18S rRNA and expressed as arbitrary units or fold increases versus normal diet mice or cell basal conditions.

2.9. Statistics

Outcome assessments and data analysis were conducted in a blinded manner. Results are presented as individual data points and mean ± SD from separate experiments and mice, with each condition analyzed in duplicate/triplicate and including the corresponding negative controls. Statistical analysis was conducted with GraphPad Prism v8 (GraphPad Software Inc, La Joya, CA, USA). Data were assessed for normality (D'Agostino and Pearson test) and variance homogeneity (Bartlett test). Pearson's correlation was used for normally distributed data. Statistical significance was set at $P < 0.05$ using one- or two-way ANOVA with Tukey's multiple comparisons test.

3. Results

3.1. Linear S1 and liPS peptides dose-dependently attenuate early hepatic damage caused by MCD diet in mice

To evaluate SOCS1 linear mimetics in early MASLD, mice were fed an MCD diet for 3 weeks and simultaneously administered S1 or liPS (0.6 and 1.2 nmol/g). As expected [7], MCD diet reduced body and liver weight, serum glucose, cholesterol and TG levels, while increasing AST and ALT (Table 1). Compared to the vehicle control group, treated mice showed partial restoration of liver weight, serum glucose and lipids, and

Table 1
Metabolic parameters in C57BL/6 mice after 3 weeks of MCD diet feeding. Mice on MCD diet were treated with vehicle (Control), S1 or liPS peptides at the doses indicated (nmol/g body weight). Normal diet (ND) was used as reference group. Mean ± SD of the indicated number of animals per group. [a]P<0.05 vs ND; [b]P < 0.05 vs Control. Abbreviations: BW, body weight; LW, liver weight; LW/BW, relative liver-to-body weight; BG, blood glucose; ALT, alanine aminotransferase; AST, aspartate aminotransferase; Chol, total cholesterol; TG, triglycerides.

		3wk MCD				
	ND (n = 8)	**Control** (n = 8)	**S1-0.6** (n = 5)	**S1-1.2** (n = 7)	**liPS-0.6** (n = 5)	**liPS-1.2** (n = 7)
Initial BW (g)	29.0 ± 1.3	30.0 ± 1.5	29.7 ± 1.0	29.3 ± 1.1	31.6 ± 1.4	30.1 ± 0.8
Final BW (g)	29.6 ± 1.2	20.1 ± 1.3[a]	20.9 ± 0.2[a]	21.6 ± 0.9[a]	19.7 ± 1.1[a]	21.1 ± 0.9[a]
LW (g)	1.82 ± 0.08	0.94 ± 0.20[a]	1.08 ± 0.17[a]	1.28 ± 0.08[a,b]	1.10 ± 0.12[a]	1.25 ± 0.12[a,b]
LW/BW (g/g)	0.061 ± 0.002	0.047 ± 0.010[a]	0.052 ± 0.008	0.059 ± 0.004[b]	0.056 ± 0.008	0.060 ± 0.006[b]
BG (mg/dL)	136.4 ± 15.9	73.5 ± 4.9[a]	93.8 ± 3.9[a]	94.7 ± 5.8[a,b]	97.8 ± 17.7[a,b]	92.6 ± 14.9[a,b]
ALT (IU/L)	41.8 ± 9.5	299.1 ± 31.1[a]	229.5 ± 32.7[a,b]	177.2 ± 43.7[a,b]	234.2 ± 41.0[a,b]	188.8 ± 24.5[a,b]
AST (IU/L)	60.1 ± 17.6	236.6 ± 35.3[a]	191.4 ± 22.5[a,b]	151.4 ± 20.8[a,b]	187.1 ± 16.1[a,b]	170.6 ± 27.3[a,b]
Chol (mg/dL)	137.0 ± 16.5	47.4 ± 13.2[a]	62.7 ± 11.1[a]	78.6 ± 12.7[a,b]	70.2 ± 9.9[a]	84.8 ± 17.3[a,b]
TG (mg/dL)	108.3 ± 9.9	44.4 ± 8.0[a]	58.6 ± 7.5[a]	63.9 ± 10.5[a,b]	71.8 ± 7.9[a,b]	60.9 ± 12.8[a,b]

reduced transaminase levels, indicating attenuated liver damage (Table 1). Histological analysis revealed significant decreases in MASLD activity scores (steatosis, hepatocyte ballooning and lobular inflammation) in high-dose treatment groups, with no differences observed between the two peptides (Fig. 1A and B).

Livers of peptide-treated mice displayed reduced lipid droplet accumulation (ORO staining; Fig. 1, A and C), total cholesterol and TG levels (Fig. 1D and E). Immunohistochemistry (Fig. 1F) revealed that S1 and liPS at higher doses significantly reduced macrophage and T-cell content (F4/80 and CD3; Fig. 1G and H), and markers of oxidative DNA damage and lipid peroxidation (8OHdG and 4HNE; Fig. 1I and J). Treatment also attenuated hepatic STAT phosphorylation/activation (P-STAT1/3; Fig. 2A and B). Additionally, qPCR analysis indicated that MCD feeding upregulated liver injury-related genes, including chemokines like *Ccl2*, *Ccl5* and CXC Motif Chemokine Ligand 10 (*Cxcl10*) (Fig. 2C); cytokines like interleukin-1β (*Il1b*), *Il6* and *Tnfa* (Fig. 2D); the ROS-generating enzyme *Nox1*; the ER-stress molecule C/EBP homologous protein (*Chop*) (Fig. 2E); and the scavenger receptor class B (*Cd36*) (Fig. 2F). Notably, S1 and liPS significantly downregulated these genes while upregulating antioxidant enzymes like catalase (*Cat*) and superoxide dismutase-1 (*Sod1*) (Fig. 2E); the FA β-oxidation gene carnitine palmitoyltransferase 1α (*Cpt1a*) and the ATP-binding cassette transporters (*Abca1/g1*) involved in lipid efflux (Fig. 2F), supporting the histological findings.

3.2. Therapeutic effect of peptides in advanced stages of MASLD/MASH induced by MCD diet

To assess the effects of SOCS1 peptidomimetics in an intervention model of MASLD progression, we developed a MASH-like model by feeding mice an MCD diet for 3 weeks, followed by 3 weeks of treatment with linear (S1 and liPS) and cyclic (IC and ICNal) peptides while continuing the MCD diet (Fig. 3A). We first evaluated the pharmacokinetics of fluorescent-labeled peptides after a single dose. Our previous biodistribution studies showed that intraperitoneal administration targets multiple tissues, including the liver [19,23]. In MCD-fed mice, plasma fluorescence peaked at 4–6 h and urine fluorescence at 8 h (Fig. 3B and C), with cyclic peptides showing sustained detection for up to 30 h. Plasma half-life calculations varied depending on structural modifications ($t_{1/2}$: S1, 4.1 h; liPS, 6.5 h; IC, 8.5 h; ICNal, 12.1 h; Fig. 3D).

Therapeutic administration of peptides after the onset of MCD-induced liver damage significantly restored glucose and lipid levels, reduced transaminases (Supplementary Table S2), and improved liver histomorphology, as evidenced by decreased steatosis, hepatocyte ballooning, and lobular inflammation (Fig. 3E–G). Remarkably, peptides did not exacerbate body weight loss (Supplementary Table S2) thus reinforcing their protective effect, as observed in our previous studies in diabetes models [19,20]. Treatment also reduced liver cholesterol and TG levels (Fig. 3H and I) and restored lipid transporter expression (*Cd36* and *Abcg1*; Fig. 3J) in 6 week-MCD fed mice. Although no significant differences were observed among the four peptides, ICNal appeared most effective in reducing disease severity, likely due to its enhanced stability in cellular contexts, as we previously reported [23,24].

Changes in the FA profile of liver TG were evaluated by lipidomic analysis. Compared to control MCD-fed mice, peptide-treated groups showed a significant decrease in FA composition (Fig. 4A), mainly in the saturated FA, palmitic (C16:0; Fig. 4B) and stearic (C18:0; Fig. 4C); and the monounsaturated FA, palmitoleic (C16:1n7; Fig. 4D) and oleic (C18:1n9; Fig. 4E). A similar decrease in these major FA was also observed in the hepatic non-esterified FA fraction (Supplementary Table S3). These results suggest that peptides help to counteract long-chain FA alterations in advanced MASLD.

We next investigated the effect of peptides on liver inflammation, oxidative stress and fibrosis, which are key pathogenic factors in MASLD/MASH progression [5]. At 6 weeks of MCD diet feeding, peptide treatment markedly reduced the hepatic content of macrophages, T cells, 8OHdG, and P-STAT1, compared to the intense staining observed in MCD controls (Fig. 5A and B). Treated mice also displayed reduced gene expression of chemokines and cytokines in liver tissue (Fig. 5C), and restored expression of redox balance genes (*Nox1*, *Cat*, and *Sod1*; Fig. 5D). Sirius red staining showed decreased collagen accumulation in treated mice, indicating attenuated liver fibrosis (Fig. 5A and B). This was further reflected by downregulated expression of profibrogenic markers such as collagen type I α1 (*Col1a*), α-smooth muscle actin (*Acta2*), transforming growth factor-β1 (*Tgfb*), matrix metalloproteinases (*Mmp2, 9* and *13*), and tissue MMP inhibitor-1 (*Timp1*) (Fig. 5E). Pearson analysis revealed positive correlation between P-STAT1 and profibrotic markers in all MCD groups (Supplementary Table S4), linking STAT activation with MASLD/MASH progression.

3.3. Hepatoprotective actions of peptidomimetics in MASLD/MASH mouse model induced by HFD feeding

After confirming that both linear and cyclic SOCS1 mimetics improve hepatic damage in the MCD diet-induced lean MASH model, we examined their effects in *ApoE*$^{-/-}$ mice fed an HFD for 12 weeks (Fig. 6A), a MASLD model that better represents human metabolic syndrome features such as hyperlipidemia, overweight/obesity and insulin resistance [33,34]. Compared to the untreated control group, mice receiving S1, liPS, IC, or ICNal peptides during the HFD regime showed significantly lower serum ALT, serum and hepatic TG, and fasting glucose levels (Table 2). Although food intake was not directly assessed, stable body weight in HFD-fed mice during treatment (Table 2) is consistent with our previous studies where no major changes in feeding behavior were observed [18,23]. Treatments also improved glucose tolerance, as shown by lower area under the curve values in the glucose tolerance test (Fig. 6B and C). Liver histology (Fig. 6D) revealed overall improvements

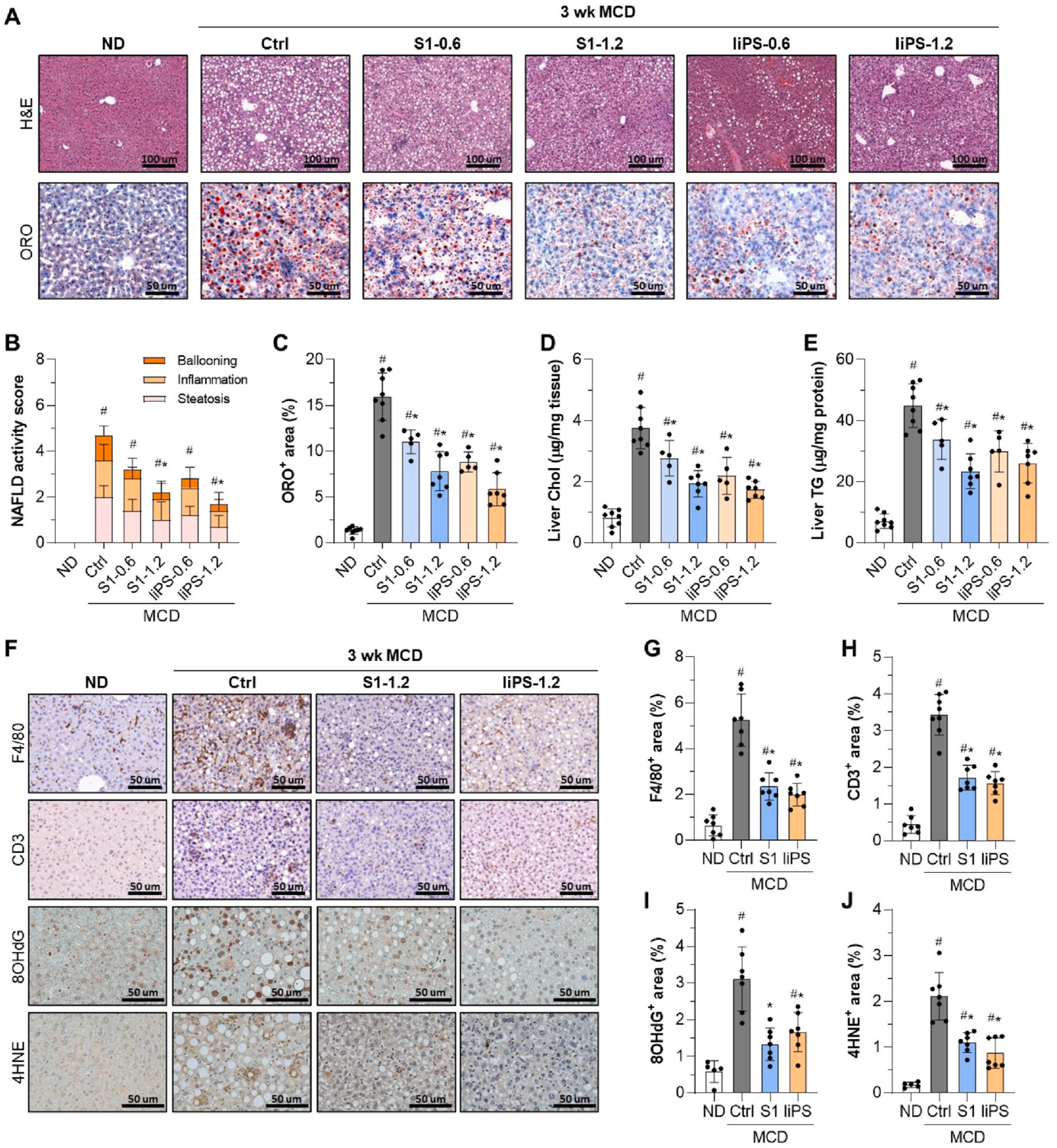

Fig. 1. Linear peptides prevent hepatic damage caused by MCD diet in mice. Mice fed an MCD diet for 3 weeks were treated with vehicle (Ctrl), S1 or liPS peptides at the doses indicated (nmol/g body weight). Normal diet (ND) was used as reference group. **(A)** Representative images of hematoxylin/eosin and ORO staining in liver samples. **(B)** Evaluation of MASLD/NAFLD activity score. **(C)** Quantification of lipid deposition. Hepatic levels of total cholesterol **(D)** and TG **(E)**. **(F)** Representative images of the immunodetection of macrophages, T cells, oxidative DNA damage and lipid peroxidation in liver sections. Quantification of F4/80 **(G)**, CD3 **(H)**, 8OHdG **(I)** and 4HNE **(J)** positive staining. Results are represented as individual data points and/or mean ± SD of the total number of animals per group. $^{\#}P < 0.05$ vs ND; $^{*}P < 0.05$ vs Ctrl.

in multiple parameters, including MASLD activity score (Fig. 6E), lipid accumulation (Fig. 6F), macrophage infiltration (Fig. 6G), oxidative stress markers (8OHdG and 4HNE; Fig. 6H), and STAT1 activation (Fig. 6I). Notably, Sirius red staining showed a 40 % reduction in collagen deposition in peptide-treated groups (Fig. 6J).

Peptides alleviated the abnormal lipidomic profile in HFD-fed mouse livers, particularly reducing palmitic, oleic, stearic, and palmitoleic acid levels in TG fractions (Fig. 7A and B). This was associated with

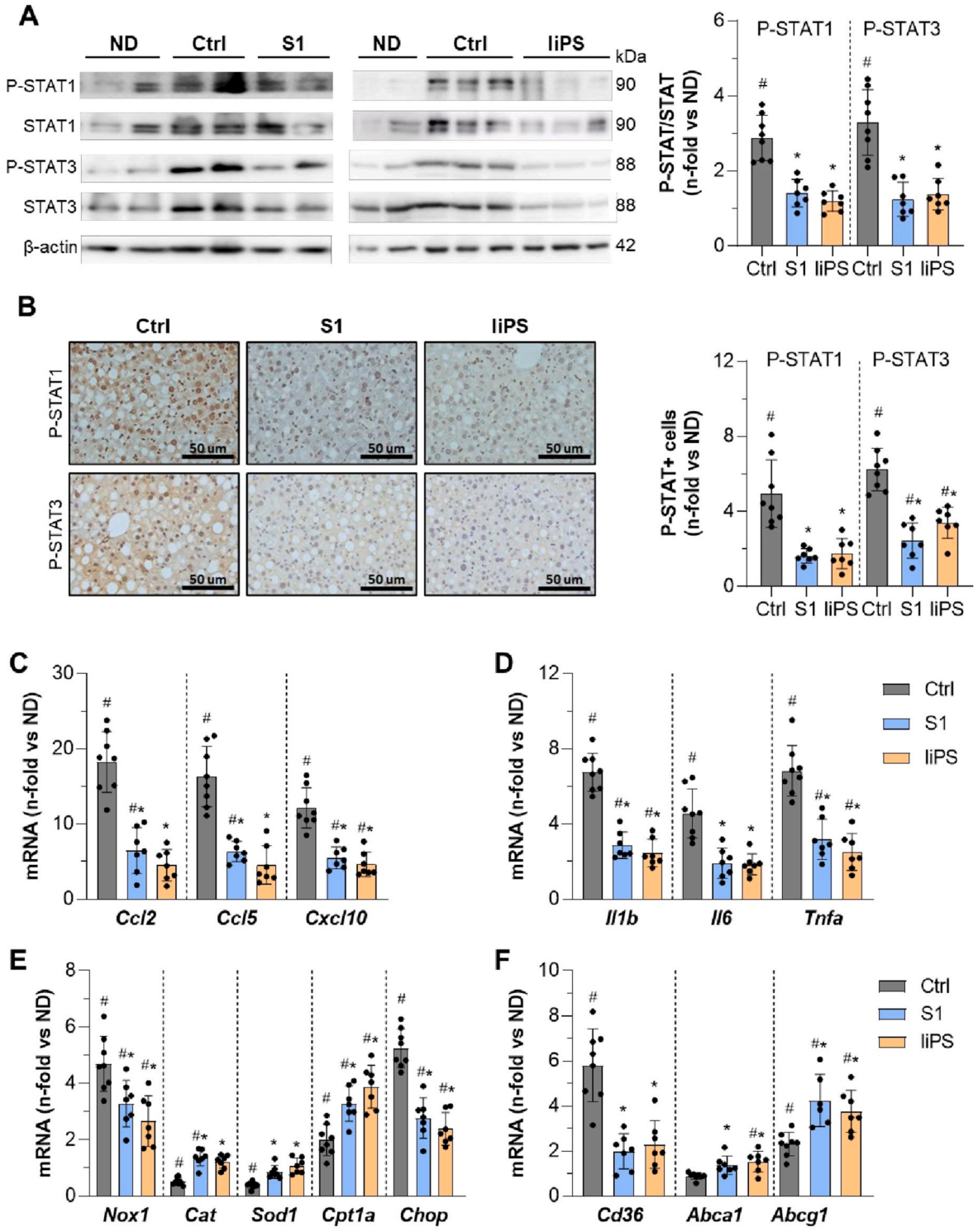

Fig. 2. S1 and liPS attenuate JAK/STAT and gene expression in livers of MCD diet-fed mice. (A) Representative immunoblots of P-STAT1/3, STAT1/3 and β-actin in liver samples from mice on MCD diet treated with vehicle (Ctrl) or peptides (S1 and liPS; 1.2 nmol/g), and normal diet (ND) as reference group. Quantitative analysis of P-STAT/STAT ratios expressed as fold increases versus ND group. **(B)** Representative images of P-STAT1/3 immunohistochemistry and quantification of positive area. Effect of peptides on MCD-induced mRNA levels of chemokines **(C)**, cytokines **(D)**, redox and ER-stress molecules **(E)**, and lipid transport genes **(F)**. The qPCR values were normalized by 18S. Results expressed as fold increases versus ND group are represented as individual data points and mean ± SD of the total number of animals per group. $^{\#}P < 0.05$ vs ND; $^{*}P < 0.05$ vs Ctrl.

downregulation of lipid transport genes such as *Cd36 and* FA-binding protein-1 (*Fabp1*) and upregulation of lipid efflux genes (*Abca1/g1*) (Fig. 7C). Treatment partially restored liver expression of genes involved in de novo lipogenesis and FA β-oxidation, including sterol regulatory element-binding transcription factor-1 (*Srebf1*), FA synthase (*Fasn*), *Cpt1a,* and peroxisome proliferator-activated receptor-gamma coactivator-1α (*Ppargc1a*) (Fig. 7D).

In HFD-fed mice, treatment with either linear or cyclic sequences attenuated hepatic expression of key inflammatory mediators, including chemokines (*Ccl2/5* and *Cxcl10*), proinflammatory cytokines (*Tnfa* and

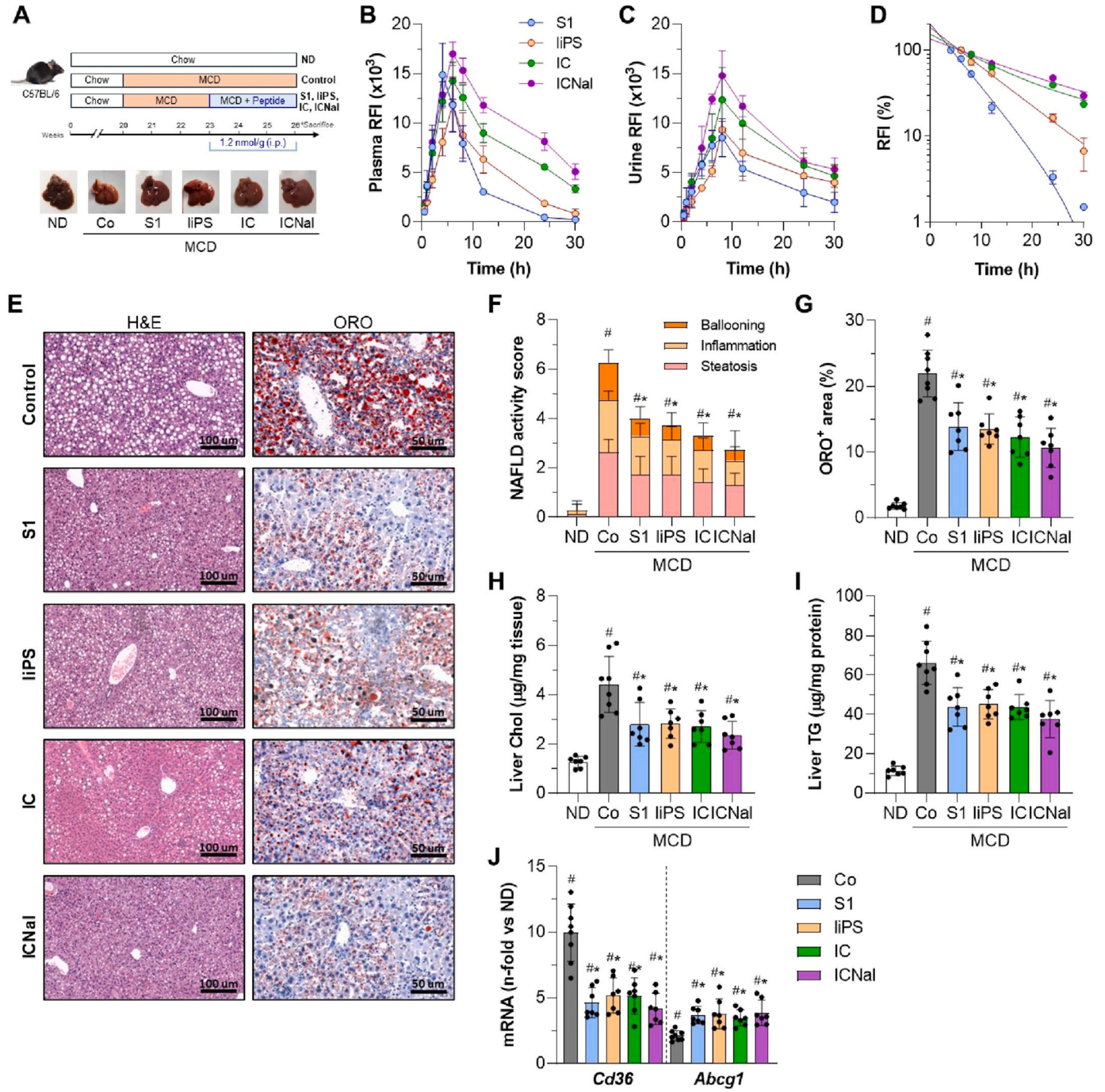

Fig. 3. Therapeutic effect of SOCS1 peptidomimetics in advanced stages of MCD diet-induced MASLD/MASH. (A) Experimental design for testing peptides in advanced MCD diet model, with representative liver images. Fluorescence analysis in plasma **(B)** and urine **(C)** after a single injection of fluorescent-labeled peptides. Values expressed as relative fluorescence (RFI; n = 2–3 per time point). **(D)** One-phase exponential regression curves of normalized plasma fluorescence. **(E)** Representative images of hematoxylin/eosin and ORO staining in liver sections from MCD-fed mice untreated (Control) and peptide-treated (S1, liPS, IC, and ICNal). **(F)** MASLD/NAFLD activity score in ND (normal diet) and MCD groups. **(G)** Quantification of lipid content. **(H)** Liver total cholesterol. **(I)** Liver TG. **(J)** Expression of lipid transport genes. The qPCR values normalized by 18S are expressed as fold increases versus ND. Values are represented as individual data points and/or mean ± SD of the total number of animals per group. $^{\#}P < 0.05$ vs ND; $^{*}P < 0.05$ vs Control (Co).

Il1b; Fig. 7E), and M1 macrophage markers (inducible NO synthase (*Nos2*) and arginase 2 (*Arg2*); Fig. 7F). Genes involved in oxidative (*Nox1*) and ER stress (*Chop*) were also affected (Fig. 7G). Conversely, peptide treatment upregulated anti-inflammatory M2 macrophage markers (*Arg1*, *Cd206*, and *Il10*; Fig. 7F) and antioxidant genes (*Sod1/2,* and *Cat*; Fig. 7G). Furthermore, a reduced expression of profibrogenic genes (*Col1a* and *Tgfb*; Fig. 7H) was observed. Significant correlations between hepatic markers and STAT1 activation was found in HFD model (Supplementary Table S5).

These findings suggest that SOCS1 peptidomimetics provide hepatoprotection against HFD-induced MASLD/MASH by regulating lipid metabolism, redox balance, inflammation and fibrogenesis.

3.4. Peptides attenuate palmitate-induced cell responses in vitro

To support the in vivo findings, we performed in vitro studies in

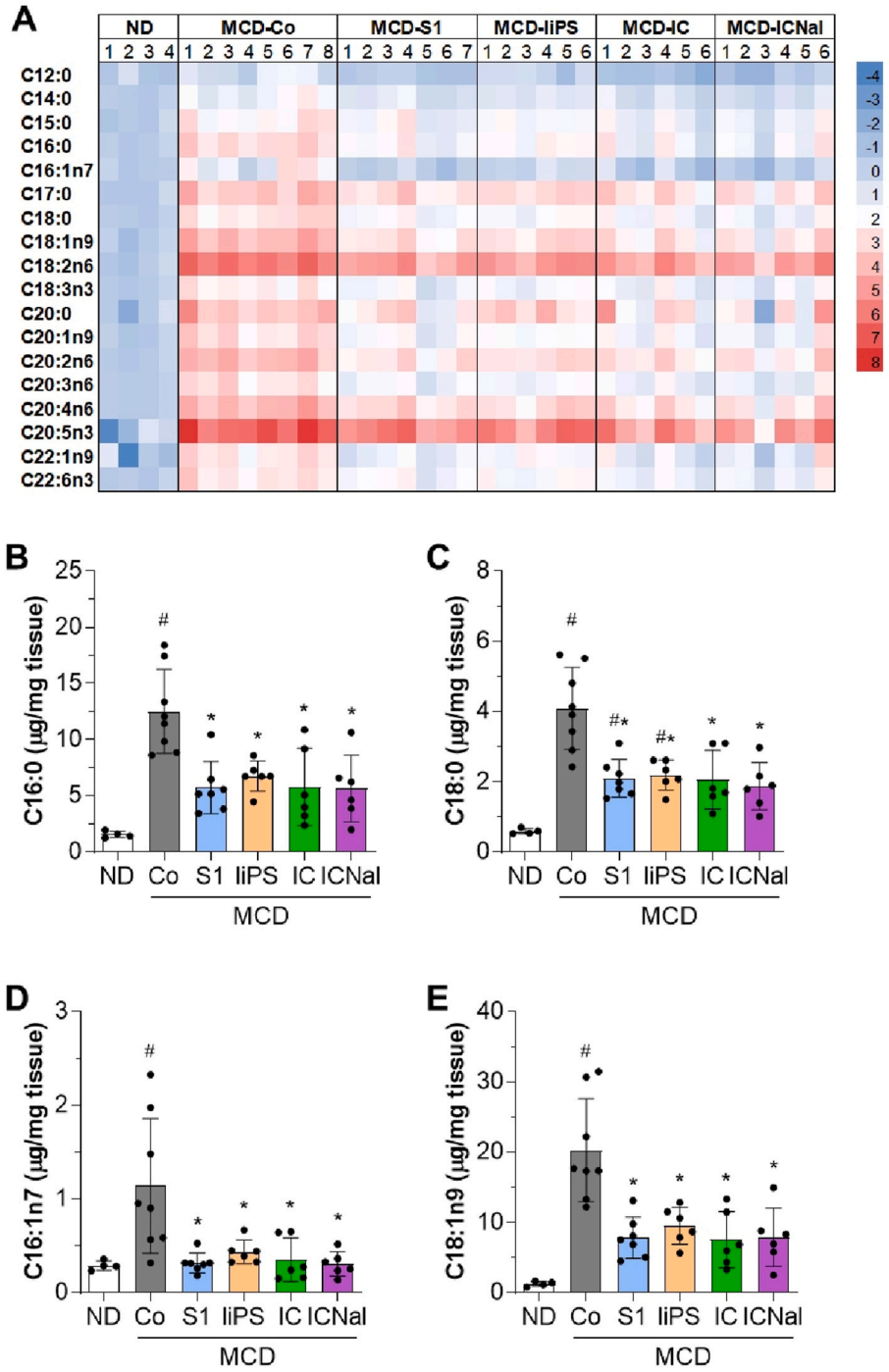

Fig. 4. FA composition of hepatic TG after 6 weeks of MCD feeding. (A) Heat-map display of quantitative analysis of individual FA in the hepatic TG fraction from MCD diet-fed mice. The color scale visualizes the log 2-fold change relative to the normal diet (ND) group. Concentrations of saturated **(B–C)** and mono-unsaturated **(D–E)** FA in hepatic TG fractions. Values are represented as individual data points and mean ± SD of the total number of animals per group. $^{\#}P < 0.05$ vs normal diet (ND); $^{*}P < 0.05$ vs Control (Co).

hepatocytes stimulated with 0.4 mM palmitate, a known lipotoxic agent. MTT assay indicated no cytotoxicity after 24 h of peptide treatment at different doses (Supplementary Fig. S3A). Notably, peptides improved the viability of lipid-treated cells (Fig. 8A). Cell-based ELISA (Fig. 8B) and Western blot (Supplementary Fig. S3B) revealed that peptides dose-dependently inhibited palmitate-induced STAT1 activation (IC_{50} ranges: S1, 45–71 µM; liPS, 21–33 µM; IC, 15–28 µM; ICNal, 11–20 µM).

Lucigenin assay in cell homogenates showed that palmitate triggered NOX-dependent ROS generation in hepatocytes, an effect significantly reduced by the peptides (Fig. 8C). Linear peptides prevented the expression of oxidative and cellular stress genes (*Nox1* and *Chop*) and upregulated antioxidant genes (*Sod1/2* and *Cat*) (Fig. 8D), whereas cyclic peptides elicited comparable, dose-dependent transcriptional effects (Fig. 8E). Additionally, peptides reduced lipid droplet accumulation (Supplementary Fig. S3C) and the expression of genes linked to lipid transport and lipogenesis while upregulating lipid metabolism genes (Fig. 8E; Supplementary Fig. S3D). Regarding inflammation, peptides reversed palmitate-induced chemokine and cytokine gene expression (Fig. 8F; Supplementary Fig. S3E), and reduced CCL2 and TNFα secretion into the culture medium (Fig. 8G).

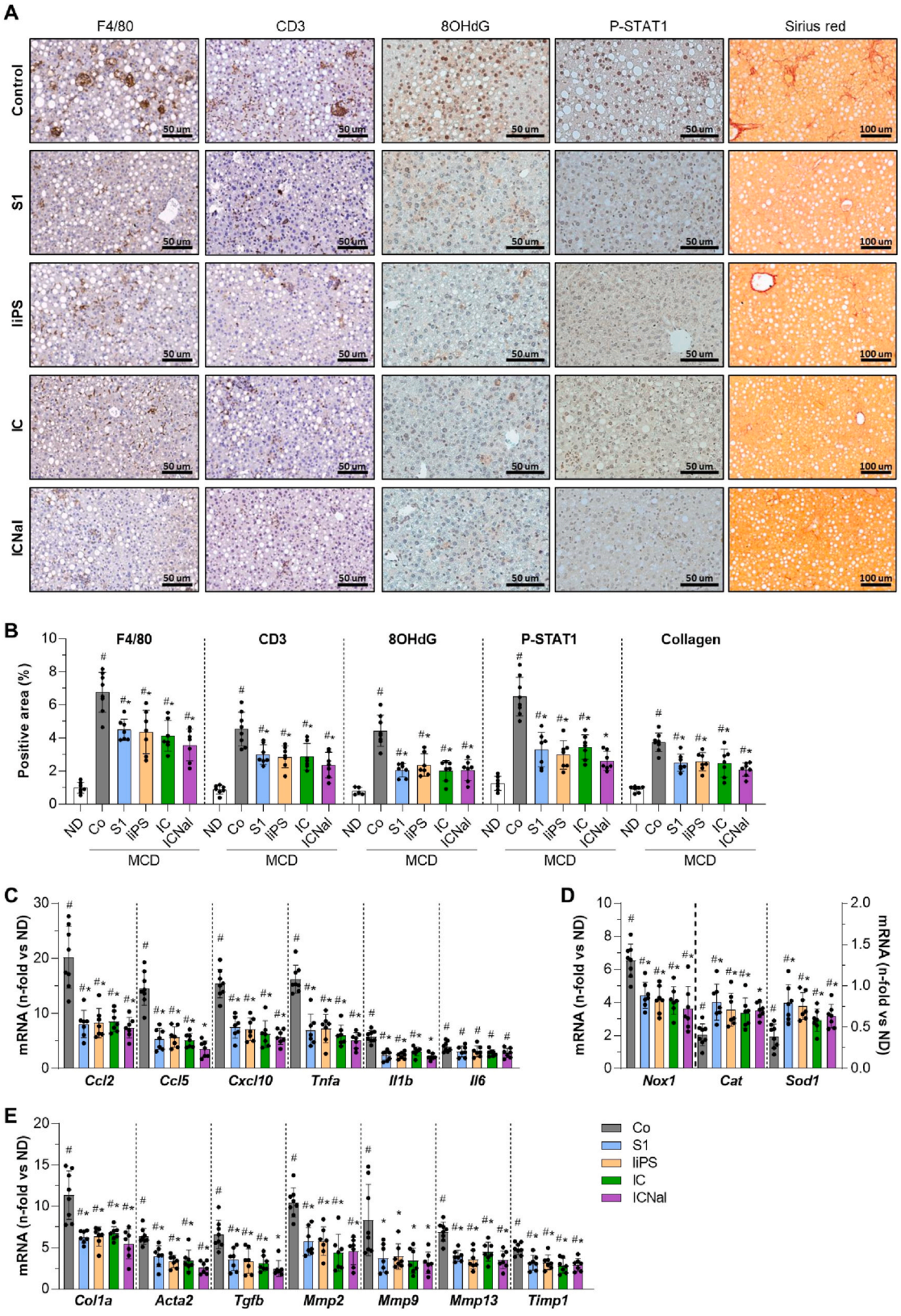

Fig. 5. Peptides reduce liver inflammation, oxidative stress, and fibrogenesis induced by MCD diet. (A) Representative images of F4/80, CD3, 8OHdG, and P-STAT1 immunoperoxidase, and Sirius red staining in liver sections from MCD diet-fed mice untreated (Control) and peptide-treated (S1, liPS, IC, and ICNal). **(B)** Quantification of positive stained area. Expression levels of inflammatory **(C)**, redox balance **(D)** and profibrotic **(E)** genes. The qPCR values normalized by 18S are expressed as fold increases versus normal diet (ND). Values are represented as individual data points and/or mean ± SD of the total number of animals per group. $^{\#}P < 0.05$ vs ND; $^{*}P < 0.05$ vs Control (Co).

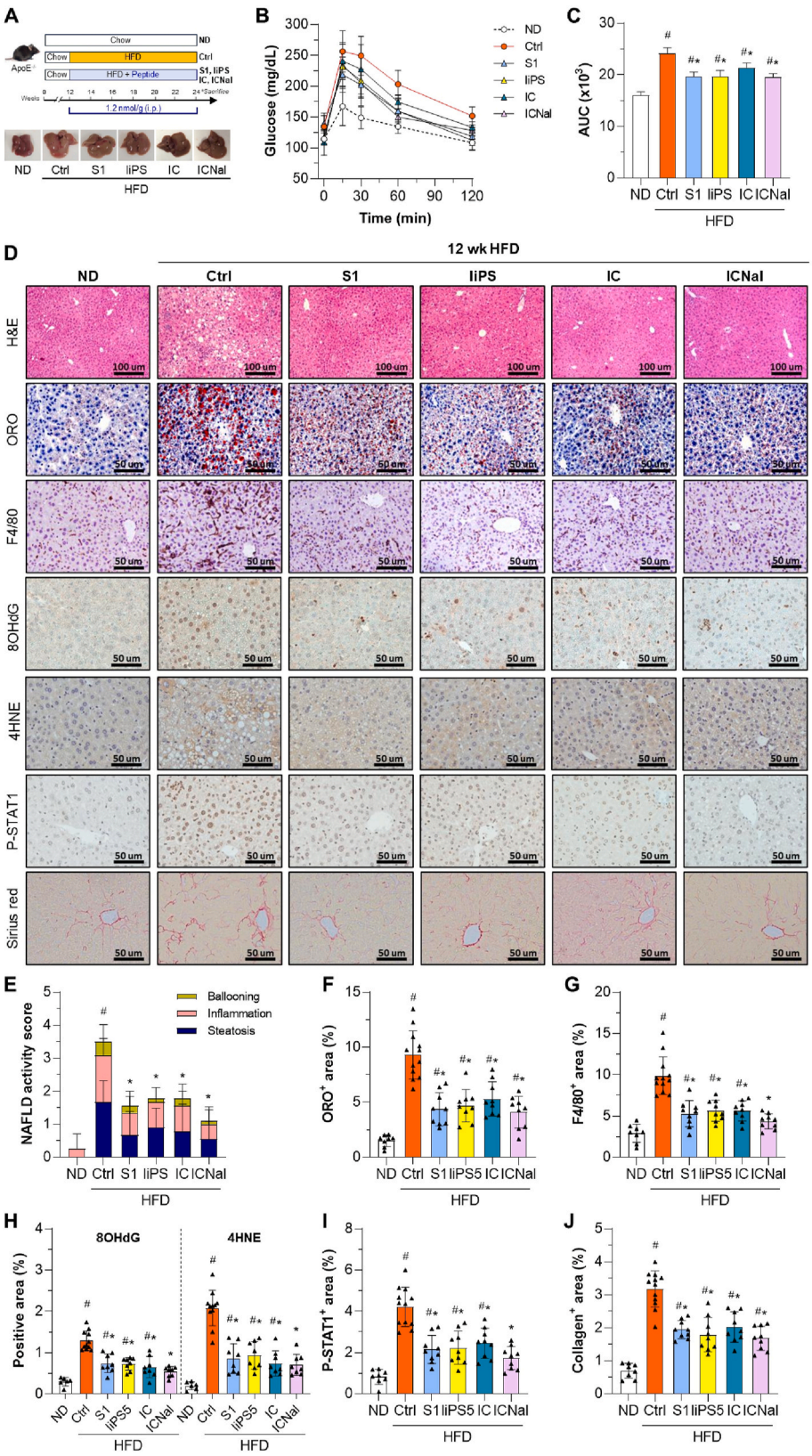

Fig. 6. Hepatoprotective effect of peptides in a mouse model of HFD-induced MASLD/MASH. (A) Experimental design for testing peptides in HFD-fed *ApoE*$^{-/-}$ mice, with representative liver images. **(B–C)** Glucose tolerance test at 11 weeks of HFD in control (Ctrl), treated (S1, liPS, IC and ICNal) mice, and age-matched ND-fed mice. Blood glucose levels over time **(B)** and area under the curve (AUC) **(C)** were measured. **(D)** Representative images of hematoxylin/eosin, ORO, F4/80, 8OHdG, 4HNE, P-STAT1, and Sirius red staining in liver sections. **(E)** MASLD/NAFLD activity score. Quantification of lipid content **(F)**, F4/80+ macrophages **(G)**, oxidative stress markers **(H)**, P-STAT1 **(I)**, and collagen content **(J)** in liver samples. Values are represented as individual data points and/or mean ± SD of the total number of animals per group. $^{\#}P < 0.05$ vs ND; $^{*}P < 0.05$ vs Ctrl.

Table 2
Biochemical parameters in *ApoE*$^{-/-}$ mice fed a chow or HFD for 12 weeks. Mean ± SD of the indicated number of animals per group. [a]P<0.05 vs ND; [b]P < 0.05 vs Control. Abbreviations: ΔBW, body weight gain; LW, liver weight; LW/BW, relative liver-to-body weight; BG, blood glucose; ALT, alanine aminotransferase; TG, triglycerides.

		12 wk HFD				
	ND (n = 8)	**Control** (n = 12)	**S1** (n = 9)	**liPS** (n = 9)	**IC** (n = 9)	**ICNal** (n = 9)
ΔBW (g)	2.9 ± 1.1	7.6 ± 1.7[a]	6.2 ± 1.8[a]	5.8 ± 1.4[a]	6.2 ± 2.2[a]	6.5 ± 1.6[a]
LW (g)	1.56 ± 0.11	1.86 ± 0.09[a]	1.76 ± 0.11[a]	1.73 ± 0.09	1.74 ± 0.17[a]	1.71 ± 0.14
LW/BW (g/g)	0.051 ± 0.003	0.061 ± 0.007[a]	0.056 ± 0.005	0.063 ± 0.004[a]	0.060 ± 0.008[a]	0.057 ± 0.005
BG (mg/dL)	123.4 ± 8.4	159.9 ± 18.7[a]	137.8 ± 21.9[b]	138.3 ± 17.1[b]	136.0 ± 9.5[b]	128.7 ± 12.2[b]
ALT (IU/L)	33.4 ± 7.4	86.5 ± 21.2[a]	44.2 ± 12.4[b]	52.3 ± 12.3[b]	48.2 ± 20.5[b]	46.1 ± 13.9[b]
Serum TG (mg/dL)	144.2 ± 26.3	252.7 ± 68.9[a]	183.2 ± 43.2[b]	182.0 ± 33.3[b]	171.7 ± 35.2[b]	191.3 ± 44.0[b]
Liver TG (μg/mg prot)	17.7 ± 7.0	42.8 ± 11.0[a]	27.7 ± 7.1[b]	23.3 ± 6.9[b]	23.9 ± 9.1[b]	21.1 ± 8.0[b]

Given the role of macrophage polarization in MASLD, we investigated whether peptides modulate hepatocyte-induced macrophage activation. Conditioned media from palmitate-treated hepatocytes upregulated cytokine and M1 markers in RAW264.7 macrophages, and effect blunted by peptide pretreatment, which also upregulated M2 markers (Fig. 8H and I). Heat inactivation of conditioned media abolished these responses (Supplementary Fig. S3F), implicating heat-sensitive, JAK/STAT-depending mediators that activate liver immune cells.

4. Discussion

The global burden of MASLD and its progression to MASH underscore the urgent need for therapies that target the key pathological mechanisms driving liver injury. This study demonstrates the hepatoprotective effects of a series of SOCS1 peptidomimetics in experimental MASLD/MASH. We provide evidence of: a) inhibition of JAK/STAT pathway and downstream effectors by hepatocyte-safe doses of linear and cyclic peptides; b) mitigation of liver damage at early and advanced stages in MASLD/MASH mouse models; c) mechanistic involvement of molecules linked to lipotoxicity, oxidative stress, inflammation, and fibrogenesis. Fig. 9 provides a schematic overview of the mechanism of action of SOCS1 peptidomimetics, highlighting their effects on JAK/STAT signaling and downstream gene regulation.

Clinical and animal studies highlight the relevance of JAK/STAT/SOCS axis in metabolic and liver diseases, making it a promising therapeutic target [35]. STAT1/3 activation is elevated in MASLD/MASH patients and experimental models, contributing to liver infiltration, fibrosis, and tumorigenesis [9,36]. SOCS1 downregulation associates with liver dysfunction [14,37,38] and promotes insulin resistance, inflammation and fibrosis when silenced in macrophages or hepatocytes [15,39–41], whereas its overexpression protects hepatocytes and exerts tumor-suppressive effects [16,17,42]. Agents that upregulate SOCS1 while suppressing cytokines (e.g., sennoside A, herbal extracts, and miR-222-3p knockdown) have reduced liver damage in models [38,43,44], supporting the therapeutic potential of SOCS1-based approaches to prevent MASLD/MASH progression.

This work demonstrates the hepatoprotective effects of SOCS1 peptidomimetics in two MASLD/MASH models. In the MCD-induced lean model, the 1.2 nmol/g dose reduced liver damage both preventively and therapeutically. The cyclic ICNal, with enhanced protease resistance [24], showed improved pharmacokinetics and efficacy in advanced stages. To better mimic human metabolic disease, compounds were also tested in HFD-fed *ApoE*$^{-/-}$ mice, where both linear and cyclic forms reduced transaminases and lipids, improved glucose tolerance, and alleviated liver pathology, suggesting hepatoprotection independent of obesity.

Intrahepatic fat accumulation, a hallmark of MASLD, results from enhanced lipid uptake and synthesis alongside reduced FA export and oxidation, leading to insulin resistance, ER stress, and liver dysfunction [3]. Our study shows that peptide administration in MASLD/MASH mouse models reduced hepatic cholesterol and TG levels, altered key saturated and monounsaturated FA (palmitic, stearic, palmitoleic and oleic), and restored lipid transport gene expression by upregulating exporters (ABCA1/G1) and downregulating importers (CD36 and FABP1). CHOP reduction linked this to ER stress [45]. In HFD mice, treatment partially normalized lipogenic and FA β-oxidation genes, including FASNα (de novo saturated FA synthesis), SREBF1 (transcriptional lipogenesis regulator), CPT1α (mitochondrial long-chain FA oxidation) and PPARGC1α (FA metabolism co-activator), which are downstream targets of JAK/STAT pathway [46–49]. Additionally, in palmitate-exposed hepatocytes, peptides reduced lipid accumulation and improved cell viability, suggesting that mimicking SOCS1 function may restore lipid homeostasis in JAK/STAT-driven lipotoxicity.

Diabetes, obesity, and dyslipidemia promote chronic low-grade inflammation with elevated proinflammatory cytokines that exacerbate liver inflammation and oxidative damage, contributing to MASLD [3]. Hepatocyte- and macrophage-derived mediators amplify the response to free FA, promoting immune cell infiltration, M1 macrophage polarization, lipogenesis, and HSC activation [50,51]. In this work, peptides improved steatosis, reduced immune cell infiltration, downregulated chemokines and cytokines, and shifted the M1/M2 ratio toward an anti-inflammatory profile. Treatment also attenuated lipid peroxidation and oxidative DNA damage, suggesting partial restoration of redox balance. In vitro, SOCS1 mimetics prevented ROS production in palmitate-treated hepatocytes. This associated with downregulation of NOX1, a key source of ROS-induced liver damage [52], and upregulation of antioxidant enzymes SOD and catalase. Our previous work in renal and vascular cells demonstrated that SOCS1 therapies reduce ROS by inhibiting JAK2 activity, thereby suppressing downstream phosphatidylinositol 3-kinase activity and NOX complex assembly, while also repressing STAT1-dependent NOX expression [23,31]. Although further research is needed to confirm these mechanisms in the context of MASLD/MASH, our results indicate that peptides affect multiple aspects of JAK/STAT-driven inflammatory and oxidative stress pathways in liver cells. Previous reports have shown that levels of TNFα, IL-1β, CCL2/5, and NOX1 associated with MASH progression, while their deletion reduces MASLD severity in experimental models [50–52]. However, pharmacological inhibition of individual targets has shown limited therapeutic benefit in MASLD despite some metabolic improvements [50,53]. Notably, we previously demonstrated that S1 peptide reduced systemic inflammation in a diabetic atherosclerosis model by decreasing circulating proinflammatory monocytes and cytokines [18], supporting its potential to restore immune homeostasis at both hepatic and systemic levels. By simultaneously modulating inflammatory and oxidative pathways, SOCS1 peptidomimetics may offer a broader and more effective approach to counteract MASLD/MASH progression.

Inflammation and oxidative stress in MASLD/MASH drive liver fibrosis, which can progress to cirrhosis and liver cancer. Damaged hepatocytes activate macrophages, which release cytokines and growth factors that induce HSC transdifferentiation into collagen-producing myofibroblasts and ECM remodeling [3,5]. In our study, MASLD/-MASH mice exhibited liver fibrosis characteristics, including collagen

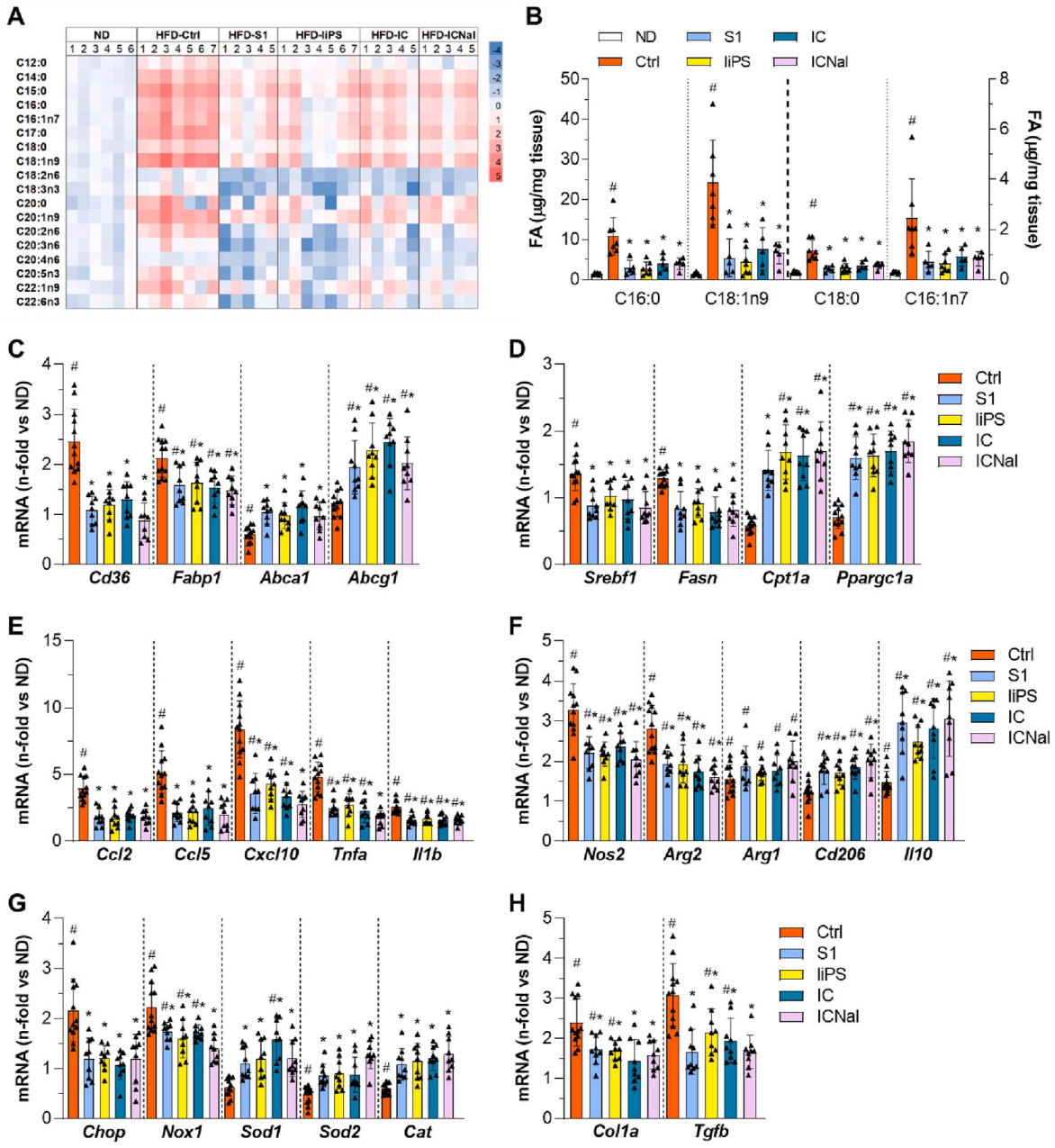

Fig. 7. Hepatic lipid composition and gene expression profile in HFD-induced MASLD/MASH. (A) Heat-map of FA quantitative analysis in the hepatic TG fractions from HFD mice untreated (Ctrl) and peptide-treated (S1, liPS, IC and ICNal). The color scale visualizes the log 2-fold change relative to the normal diet (ND) group. **(B)** Concentrations of main saturated and monounsaturated FA in mouse liver. Expression levels of genes involved in lipid transport **(C)**, lipid metabolism **(D)**, inflammation **(E)**, M1/M2 macrophage polarization **(F)**, cellular and oxidative stress **(G)**, and hepatic fibrosis **(H)**. The qPCR values normalized by 18S are expressed as fold increases versus normal diet (ND). Values are represented as individual data points and mean ± SD of the total number of animals per group. $^{\#}P < 0.05$ vs ND; $^{*}P < 0.05$ vs Ctrl.

deposition, elevated ACTA2 (myofibroblast differentiation factor) and TGFβ (profibrogenic mediator that activates HSCs and regulates ECM deposition). Peptide treatment attenuated these markers and restored the balance between ECM-degrading enzymes and their inhibitors. Previous studies have shown that modulating TGFβ and MMP activity limits ECM accumulation and promotes fibrosis resolution [54,55]. Our findings suggest SOCS1 mimetics may modulate fibrogenesis in MASLD/MASH, although further studies are needed to assess their effects in advanced fibrosis, where effective therapies are lacking.

A key advantage of our compounds is their mimicry of the natural SOCS1 KIR domain, which selectively binds the JAK activation loop and blocks substrate phosphorylation without affecting ATP binding [56]. Unlike the full-length SOCS1 protein, which contains domains like SH2 and SOCS box involved in substrate targeting and proteasomal degradation [12,56], KIR-based peptides lack these motifs, minimizing interference with broader metabolic pathways such as insulin signaling. SOCS1 mimetics specifically target JAK1/2, acting as potent and selective inhibitors with fewer off-target kinase interactions. In contrast, commercial JAK inhibitors used in rheumatoid arthritis and thrombocytopenia, target the conserved ATP-binding site, and then carry a higher risk of off-target toxicity and have been linked to cardiovascular events, despite some have shown efficacy in liver disease models [57–59]. S1 peptide has demonstrated cardiovascular safety in diabetic mice (unpublished) and protective effects in models of renal and

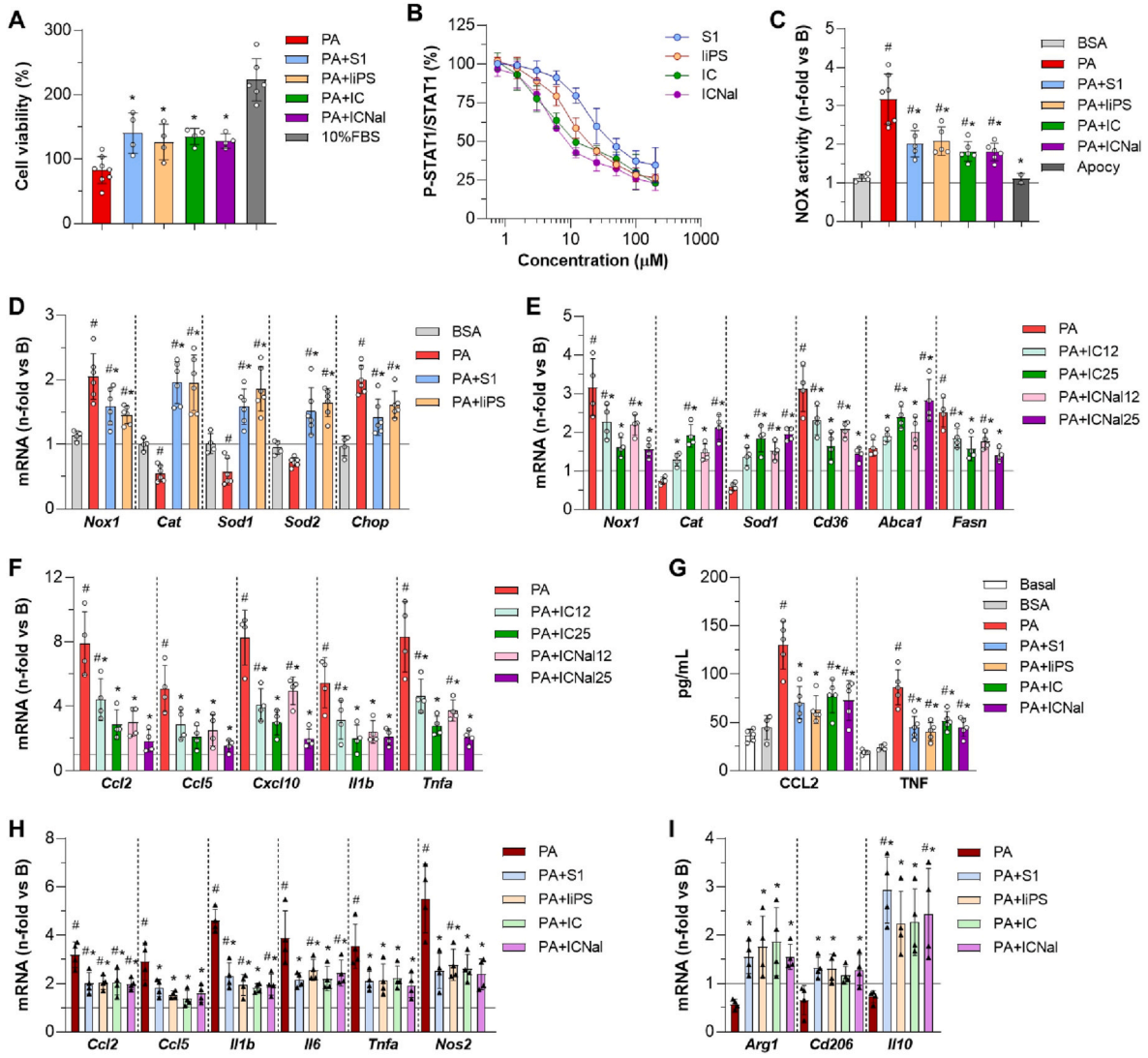

Fig. 8. Effects of linear and cyclic peptides in vitro. (A) Cell viability MTT assay in hepatocytes treated with 0.4 mM palmitic acid (PA) with/without peptides (S1, 59 μM; liPS, IC and ICNal, 25 μM). Medium with 10 % FBS was used as positive control. **(B)** Cell-based ELISA assay for STAT1 activation in hepatocytes stimulated with PA for 6 h in the presence of increasing concentrations of peptides. Values expressed as ratio P-STAT1/STAT1 versus PA alone. **(C)** NOX-dependent measurement of O2•− in hepatocytes after 16 h of stimulation, assessed by chemiluminescence assay. BSA and apocynin were used as controls. Lucigenin relative units are expressed as fold increases versus basal conditions. **(D–F)** Expression levels of redox, cell stress, lipid metabolism, and inflammatory genes in hepatocytes pretreated with peptides (S1, 59 μM; liPS, 25 μM; IC/ICNal, 12 and 25 μM) before stimulation with PA for 6 h **(D)** and 24 h **(E and F)**. **(G)** ELISA analysis of cytokine concentrations in hepatocyte conditioned media after 24 h of stimulation. Gene expression of M1 **(H)** and M2 **(I)** markers in macrophages incubated for 24 h with conditioned media from hepatocytes stimulated with PA with/without peptides. The qPCR values normalized by 18S are expressed as fold increases versus basal conditions. Results are represented as individual data points and/or mean ± SD of n = 4–6 independent experiments. $^{\#}P < 0.05$ vs basal; $^{*}P < 0.05$ vs PA.

vascular injury [18,21]. Structural modifications, such as cyclization and non-native amino acids, have enhanced affinity, solubility, and protease resistance [22–24], supporting peptide potential as effective and safer treatment for MASLD and related conditions.

5. Conclusion

We demonstrate that SOCS1 mimetic peptides attenuate hepatic damage in experimental MASLD/MASH by restoring the balance of lipid metabolism, inflammation, oxidative stress, and fibrogenesis. Our results provide proof-of-concept and support the preclinical development of these compounds as potential treatment for MASLD patients.

CRediT authorship contribution statement

Susana Bernal: Writing – review & editing, Methodology, Investigation, Formal analysis. **Ignacio Prieto:** Writing – review & editing, Methodology, Investigation, Formal analysis. **María Kavanagh:** Writing – review & editing, Validation, Methodology, Formal analysis, Data curation. **Isabel Herrero del Real:** Writing – review & editing, Validation, Methodology, Formal analysis, Data curation. **Sara La Manna:** Writing – review & editing, Methodology, Investigation, Conceptualization. **Iolanda Lázaro:** Writing – review & editing, Validation, Methodology, Formal analysis, Data curation. **Hernán Quiceno:** Validation, Methodology, Formal analysis, Data curation. **Laura López-Sanz:** Writing – review & editing, Validation, Methodology, Formal analysis, Data curation. **Belén Picatoste:** Resources, Methodology. **M. Pilar Valdecantos:** Writing – review & editing, Resources, Methodology. **Sebastián Mas-Fontao:** Writing – review & editing, Resources, Methodology. **Aleix Sala-Vila:** Writing – review & editing, Validation, Methodology, Formal analysis, Data curation. **Ángela M. Valverde:** Writing – review & editing, Resources, Methodology. **Daniela Marasco:**

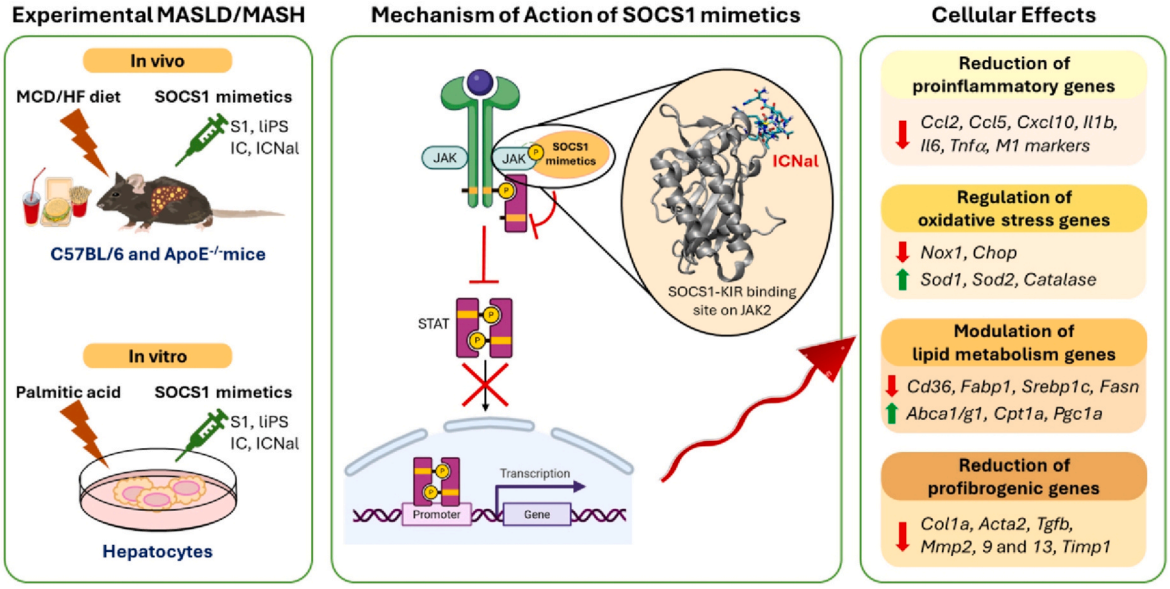

Fig. 9. Mechanism of action of SOCS1 mimetics in experimental MASLD/MASH. Schematic representation of JAK2 interaction and downstream effects on gene expression. JAK2/peptide interaction modelling adapted from [24].

Writing – review & editing, Methodology, Investigation, Conceptualization. **Jesús Egido:** Writing – review & editing, Supervision, Funding acquisition, Conceptualization. **Carmen Gómez-Guerrero:** Writing – review & editing, Writing – original draft, Methodology, Investigation, Funding acquisition, Data curation, Conceptualization.

Funding

This study was supported by MICIU/AEI/10.13039/501100011033 and "ERDF/EU" (grant PID2021-127741OB-I00 to CGG), Instituto de Salud Carlos III (grants DTS19/00093 and PI23/00119 to JE) and CIBERDEM (postdoctoral contract to IP). We thank Comunidad de Madrid and UAM for supporting MK (PIPF-2023-SAL-GL-29901) and IHR (PEJ-2023-AI_SAL-GL-28534). DM was supported by Associazione Italiana per la Ricerca sul Cancro (AIRC; grant IG 2022, Rif. 27378). AMV is member of COMETA network (CSIC, Spain).

Declaration of competing interest

The authors declare the following financial interests/personal relationships which may be considered as potential competing interests: Carmen Gomez-Guerrero (as corresponding author), Ignacio Prieto, Susana Bernal, Sara La Manna, Daniela Marasco, Laura Lopez-Sanz, Sebastian Mas-Fontao, and Jesus Egido (as co-authors) have patent #PCT/EP2023/079934 pending to Assignee: IIS-Fundación Jiménez Díaz, Autonomous University of Madrid and CIBERDEM. If there are other authors, they declare that they have no known competing financial interests or personal relationships that could have appeared to influence the work reported in this paper.

Acknowledgement

The authors gratefully acknowledge Lucas Opazo, Marisa Pardines, and the animal facility staff (IIS-Fundacion Jimenez Diaz, Madrid) for their advice and collaboration.

Appendix A. Supplementary data

Supplementary data to this article can be found online at https://doi.org/10.1016/j.redox.2025.103670.

Data availability

Data will be made available on request.

References

[1] M.E. Rinella, J.V. Lazarus, V. Ratziu, et al., A multisociety Delphi consensus statement on new fatty liver disease nomenclature, J. Hepatol. 79 (6) (2023) 1542–1556, https://doi.org/10.1016/j.jhep.2023.06.003.
[2] A.M. Allen, Z.M. Younossi, A.M. Diehl, et al., Envisioning how to advance the MASH field, Nat. Rev. Gastroenterol. Hepatol. (2024), https://doi.org/10.1038/s41575-024-00938-9.
[3] M. Noureddin, A.J. Sanyal, Pathogenesis of NASH: the impact of multiple pathways, Curr. Hepat. Rep. 17 (4) (2018) 350–360, https://doi.org/10.1007/s11901-018-0425-7.
[4] E. Buzzetti, M. Pinzani, E.A. Tsochatzis, The multiple-hit pathogenesis of non-alcoholic fatty liver disease (NAFLD), Metabolism 65 (8) (2016) 1038–1048, https://doi.org/10.1016/j.metabol.2015.12.012.
[5] S. Kumar, Q. Duan, R. Wu, et al., Pathophysiological communication between hepatocytes and non-parenchymal cells in liver injury from NAFLD to liver fibrosis, Adv. Drug Deliv. Rev. 176 (2021) 113869, https://doi.org/10.1016/j.addr.2021.113869.
[6] T. Puengel, F. Tacke, Pharmacotherapeutic options for metabolic dysfunction-associated steatotic liver disease: where are we today? Expet Opin. Pharmacother. (2024) 1–15, https://doi.org/10.1080/14656566.2024.2374463.
[7] K. Stephenson, L. Kennedy, L. Hargrove, et al., Updates on dietary models of nonalcoholic fatty liver disease: current studies and insights, Gene Expr. 18 (1) (2018) 5–17, https://doi.org/10.3727/105221617x15093707969658.
[8] L. Parlati, M. Régnier, H. Guillou, et al., New targets for NAFLD, JHEP Rep. 3 (6) (2021) 100346, https://doi.org/10.1016/j.jhepr.2021.100346.
[9] D.W. Dodington, H.R. Desai, M. Woo, JAK/STAT - emerging players in metabolism, Trends Endocrinol. Metabol. 29 (1) (2018) 55–65, https://doi.org/10.1016/j.tem.2017.11.001.
[10] X. Kong, N. Horiguchi, M. Mori, et al., Cytokines and STATs in liver fibrosis, Front. Physiol. 3 (2012) 69, https://doi.org/10.3389/fphys.2012.00069.
[11] J. Liu, F. Wang, F. Luo, The role of JAK/STAT pathway in fibrotic diseases: molecular and cellular mechanisms, Biomolecules 13 (1) (2023), https://doi.org/10.3390/biom13010119.
[12] G.A. Durham, J.J.L. Williams, M.T. Nasim, et al., Targeting SOCS proteins to control JAK-STAT signalling in disease, Trends Pharmacol. Sci. 40 (5) (2019) 298–308, https://doi.org/10.1016/j.tips.2019.03.001.
[13] A. Kempinska-Podhorodecka, E. Wunsch, P. Milkiewicz, et al., The association between SOCS1-1656g>A polymorphism, insulin resistance and obesity in nonalcoholic fatty liver disease (NAFLD) patients, J. Clin. Med. 8 (11) (2019), https://doi.org/10.3390/jcm8111912.
[14] L. Tan, W. Jiang, A. Lu, et al., miR-155 aggravates liver ischemia/reperfusion injury by suppressing SOCS1 in mice, Transplant. Proc. 50 (10) (2018) 3831–3839, https://doi.org/10.1016/j.transproceed.2018.08.060.
[15] E.K. Mafanda, R. Kandhi, D. Bobbala, et al., Essential role of suppressor of cytokine signaling 1 (SOCS1) in hepatocytes and macrophages in the regulation of liver

fibrosis, Cytokine 124 (2019) 154501, https://doi.org/10.1016/j.cyto.2018.07.032.
[16] R. Kandhi, A. Menendez, S. Ramanathan, et al., Regulation of high-fat diet-induced liver fibrosis by SOCS1 expression in hepatic stellate cells, J. Clin. Exp. Hepatol. 14 (1) (2024) 101280, https://doi.org/10.1016/j.jceh.2023.09.001.
[17] M.G.M. Khan, N. Boufaied, M. Yeganeh, et al., SOCS1 deficiency promotes hepatocellular carcinoma via SOCS3-dependent CDKN1A induction and NRF2 activation, Cancers (Basel) 15 (3) (2023), https://doi.org/10.3390/cancers15030905.
[18] C. Recio, A. Oguiza, I. Lazaro, et al., Suppressor of cytokine signaling 1-derived peptide inhibits Janus kinase/signal transducers and activators of transcription pathway and improves inflammation and atherosclerosis in diabetic mice, Arterioscler. Thromb. Vasc. Biol. 34 (9) (2014) 1953–1960.
[19] C. Recio, I. Lazaro, A. Oguiza, et al., Suppressor of cytokine signaling-1 peptidomimetic limits progression of diabetic nephropathy, J. Am. Soc. Nephrol. 28 (2) (2017) 575–585.
[20] L. Opazo-Ríos, Y. Sanchez Matus, R.R. Rodrigues-Díez, et al., Anti-inflammatory, antioxidant and renoprotective effects of SOCS1 mimetic peptide in the BTBR ob/ob mouse model of type 2 diabetes, BMJ Open Diabetes Res. Care 8 (1) (2020), https://doi.org/10.1136/bmjdrc-2020-001242.
[21] S. Bernal, L. Lopez-Sanz, L. Jimenez-Castilla, et al., Protective effect of suppressor of cytokine signalling 1-based therapy in experimental abdominal aortic aneurysm, Br. J. Pharmacol. (2020), https://doi.org/10.1111/bph.15330.
[22] S. La Manna, L. Lopez-Sanz, M. Leone, et al., Structure-activity studies of peptidomimetics based on kinase-inhibitory region of suppressors of cytokine signaling 1, Biopolymers (2017), https://doi.org/10.1002/bip.23082.
[23] S. La Manna, L. Lopez-Sanz, S. Bernal, et al., Antioxidant effects of PS5, a peptidomimetic of suppressor of cytokine signaling 1, in experimental atherosclerosis, Antioxidants 9 (8) (2020), https://doi.org/10.3390/antiox9080754.
[24] S. La Manna, L. Lopez-Sanz, S. Bernal, et al., Cyclic mimetics of kinase-inhibitory region of Suppressors of Cytokine Signaling 1: progress toward novel anti-inflammatory therapeutics, Eur. J. Med. Chem. 221 (2021) 113547, https://doi.org/10.1016/j.ejmech.2021.113547.
[25] J. Folch, M. Lees, G.H. Sloane Stanley, A simple method for the isolation and purification of total lipides from animal tissues, J. Biol. Chem. 226 (1) (1957) 497–509.
[26] M. Soto-Catalán, L. Opazo-Ríos, H. Quiceno, et al., Semaglutide improves liver steatosis and de novo lipogenesis markers in obese and type-2-diabetic mice with metabolic-dysfunction-associated steatotic liver disease, Int. J. Mol. Sci. 25 (5) (2024), https://doi.org/10.3390/ijms25052961.
[27] W. Liang, A.L. Menke, A. Driessen, et al., Establishment of a general NAFLD scoring system for rodent models and comparison to human liver pathology, PLoS One 9 (12) (2014) e115922, https://doi.org/10.1371/journal.pone.0115922.
[28] B. Picatoste, E. Ramírez, A. Caro-Vadillo, et al., Sitagliptin reduces cardiac apoptosis, hypertrophy and fibrosis primarily by insulin-dependent mechanisms in experimental type-II diabetes. Potential roles of GLP-1 isoforms, PLoS One 8 (10) (2013) e78330, https://doi.org/10.1371/journal.pone.0078330.
[29] V. Pardo, Á. González-Rodríguez, C. Guijas, et al., Opposite cross-talk by oleate and palmitate on insulin signaling in hepatocytes through macrophage activation, J. Biol. Chem. 290 (18) (2015) 11663–11677, https://doi.org/10.1074/jbc.M115.649483.
[30] R. Belfort, S.A. Harrison, K. Brown, et al., A placebo-controlled trial of pioglitazone in subjects with nonalcoholic steatohepatitis, N. Engl. J. Med. 355 (22) (2006) 2297–2307, https://doi.org/10.1056/NEJMoa060326.
[31] L. Lopez-Sanz, S. Bernal, C. Recio, et al., SOCS1-targeted therapy ameliorates renal and vascular oxidative stress in diabetes via STAT1 and PI3K inhibition, Lab. Invest. 98 (10) (2018) 1276–1290, https://doi.org/10.1038/s41374-018-0043-6.
[32] I. Prieto, M. Kavanagh, L. Jimenez-Castilla, et al., A mutual regulatory loop between miR-155 and SOCS1 influences renal inflammation and diabetic kidney disease, Mol. Ther. Nucleic Acids 34 (2023) 102041, https://doi.org/10.1016/j.omtn.2023.102041.
[33] R. Schierwagen, L. Maybüchen, S. Zimmer, et al., Seven weeks of Western diet in apolipoprotein-E-deficient mice induce metabolic syndrome and non-alcoholic steatohepatitis with liver fibrosis, Sci. Rep. 5 (2015) 12931, https://doi.org/10.1038/srep12931.
[34] F.N. Camargo, S.L. Matos, L.C.C. Araujo, et al., Western diet-fed ApoE knockout male mice as an experimental model of non-alcoholic steatohepatitis, Curr. Issues Mol. Biol. 44 (10) (2022) 4692–4703, https://doi.org/10.3390/cimb44100320.
[35] G.Y. Wang, X.Y. Zhang, C.J. Wang, et al., Emerging novel targets for nonalcoholic fatty liver disease treatment: evidence from recent basic studies, World J. Gastroenterol. 29 (1) (2023) 75–95, https://doi.org/10.3748/wjg.v29.i1.75.
[36] M. Grohmann, F. Wiede, G.T. Dodd, et al., Obesity drives STAT-1-dependent NASH and STAT-3-dependent HCC, Cell 175 (5) (2018) 1289, https://doi.org/10.1016/j.cell.2018.09.053, 306.e20.
[37] S.S. Li, M. Yang, Y.P. Chen, et al., Dendritic cells with increased expression of suppressor of cytokine signaling 1(SOCS1) gene ameliorate lipopolysaccharide/d-galactosamine-induced acute liver failure, Mol. Immunol. 101 (2018) 10–18, https://doi.org/10.1016/j.molimm.2018.05.016.
[38] P. Zhang, J. Yu, Y. Gui, et al., Inhibition of miRNA-222-3p relieves staphylococcal enterotoxin B-induced liver inflammatory injury by upregulating suppressors of cytokine signaling 1, Yonsei Med. J. 60 (11) (2019) 1093–1102, https://doi.org/10.3349/ymj.2019.60.11.1093.
[39] C. Cheng, C. Huang, T.T. Ma, et al., SOCS1 hypermethylation mediated by DNMT1 is associated with lipopolysaccharide-induced inflammatory cytokines in macrophages, Toxicol. Lett. 225 (3) (2014) 488–497, https://doi.org/10.1016/j.toxlet.2013.12.023.
[40] Z. Hu, Y. Li, W. Yuan, et al., N6-methyladenosine of Socs1 modulates macrophage inflammatory response in different stiffness environments, Int. J. Biol. Sci. 18 (15) (2022) 5753–5769, https://doi.org/10.7150/ijbs.74196.
[41] N. Sachithanandan, K.L. Graham, S. Galic, et al., Macrophage deletion of SOCS1 increases sensitivity to LPS and palmitic acid and results in systemic inflammation and hepatic insulin resistance, Diabetes 60 (8) (2011) 2023–2031, https://doi.org/10.2337/db11-0259.
[42] G. Sass, N.D. Shembade, G. Tiegs, Tumour necrosis factor alpha (TNF)-TNF receptor 1-inducible cytoprotective proteins in the mouse liver: relevance of suppressors of cytokine signalling, Biochem. J. 385 (Pt 2) (2005) 537–544, https://doi.org/10.1042/bj20040279.
[43] H. Zhu, H. Zhao, S. Xu, et al., Sennoside A alleviates inflammatory responses by inhibiting the hypermethylation of SOCS1 in CCl(4)-induced liver fibrosis, Pharmacol. Res. 174 (2021) 105926, https://doi.org/10.1016/j.phrs.2021.105926.
[44] Y. Zhang, X. Zhu, D. Zheng, et al., Effects of qutan huoxue formula on the SOCS1/TLR4 signaling pathway in NASH model mice, Evid Based Comple. Alternat. Med. 2020 (2020) 1570918, https://doi.org/10.1155/2020/1570918.
[45] J.A. Willy, S.K. Young, J.L. Stevens, et al., CHOP links endoplasmic reticulum stress to NF-κB activation in the pathogenesis of nonalcoholic steatohepatitis, Mol. Biol. Cell 26 (12) (2015) 2190–2204, https://doi.org/10.1091/mbc.E15-01-0036.
[46] Y. Gosmain, N. Dif, V. Berbe, et al., Regulation of SREBP-1 expression and transcriptional action on HKII and FAS genes during fasting and refeeding in rat tissues, J. Lipid Res. 46 (4) (2005) 697–705, https://doi.org/10.1194/jlr.M400261-JLR200.
[47] Y.F. Song, K. Wu, X.Y. Tan, et al., Effects of recombinant human leptin administration on hepatic lipid metabolism in yellow catfish Pelteobagrus fulvidraco: in vivo and in vitro studies, Gen. Comp. Endocrinol. 212 (2015) 92–99, https://doi.org/10.1016/j.ygcen.2015.01.022.
[48] R. Hashimoto, R. Kakigi, Y. Miyamoto, et al., JAK-STAT-dependent regulation of scavenger receptors in LPS-activated murine macrophages, Eur. J. Pharmacol. 871 (2020) 172940, https://doi.org/10.1016/j.ejphar.2020.172940.
[49] X.R. Hao, D.L. Cao, Y.W. Hu, et al., IFN-gamma down-regulates ABCA1 expression by inhibiting LXRalpha in a JAK/STAT signaling pathway-dependent manner, Atherosclerosis 203 (2) (2009) 417–428, https://doi.org/10.1016/j.atherosclerosis.2008.07.029.
[50] I.D. Vachliotis, S.A. Polyzos, The role of tumor necrosis factor-alpha in the pathogenesis and treatment of nonalcoholic fatty liver disease, Curr. Obes. Rep 12 (3) (2023) 191–206, https://doi.org/10.1007/s13679-023-00519-y.
[51] V. Ajmera, E.R. Perito, N.M. Bass, et al., Novel plasma biomarkers associated with liver disease severity in adults with nonalcoholic fatty liver disease, Hepatology 65 (1) (2017) 65–77, https://doi.org/10.1002/hep.28776.
[52] M. Matsumoto, J. Zhang, X. Zhang, et al., The NOX1 isoform of NADPH oxidase is involved in dysfunction of liver sinusoids in nonalcoholic fatty liver disease, Free Radic. Biol. Med. 115 (2018) 412–420, https://doi.org/10.1016/j.freeradbiomed.2017.12.019.
[53] Q.M. Anstee, B.A. Neuschwander-Tetri, V. Wai-Sun Wong, et al., Cenicriviroc lacked efficacy to treat liver fibrosis in nonalcoholic steatohepatitis: AURORA phase III randomized study, Clin. Gastroenterol. Hepatol. 22 (1) (2024) 124, https://doi.org/10.1016/j.cgh.2023.04.003, 34.e1.
[54] E. Roeb, Matrix metalloproteinases and liver fibrosis (translational aspects), Matrix Biol. 68–69 (2018) 463–473, https://doi.org/10.1016/j.matbio.2017.12.012.
[55] H. Ahmed, M.I. Umar, S. Imran, et al., TGF-β1 signaling can worsen NAFLD with liver fibrosis backdrop, Exp. Mol. Pathol. 124 (2022) 104733, https://doi.org/10.1016/j.yexmp.2021.104733.
[56] N.P.D. Liau, A. Laktyushin, I.S. Lucet, et al., The molecular basis of JAK/STAT inhibition by SOCS1, Nat. Commun. 9 (1) (2018) 1558, https://doi.org/10.1038/s41467-018-04013-1.
[57] S. Al-Fayoumi, T. Hashiguchi, Y. Shirakata, et al., Pilot study of the antifibrotic effects of the multikinase inhibitor pacritinib in a mouse model of liver fibrosis, J. Exp. Pharmacol. 10 (2018) 9–17, https://doi.org/10.2147/jep.S150729.
[58] S. Torres, C. Ortiz, N. Bachtler, et al., Janus kinase 2 inhibition by pacritinib as potential therapeutic target for liver fibrosis, Hepatology 77 (4) (2023) 1228–1240, https://doi.org/10.1002/hep.32746.
[59] Z. Song, X. Liu, W. Zhang, et al., Ruxolitinib suppresses liver fibrosis progression and accelerates fibrosis reversal via selectively targeting Janus kinase 1/2, J. Transl. Med. 20 (1) (2022) 157, https://doi.org/10.1186/s12967-022-03366-y.